How Far Can You Reach?

Ciprian Borcea
Rider University

Ileana Streinu
Smith College, istreinu@smith.edu

How far can you reach?

Ciprian Borcea [1] and Ileana Streinu [2]

Abstract

The problem of computing the maximum reach configurations of a 3D revolute-jointed manipulator is a long-standing open problem in robotics. In this paper we present an optimal algorithmic solution for orthogonal polygonal chains. This appears as a special case of a larger family, fully characterized here by a technical condition. Until now, in spite of the practical importance of the problem, only numerical optimization heuristics were available, with no guarantee of obtaining the global maximum. In fact, the problem was not even known to be computationally solvable, and in practice, the numerical heuristics were applicable only to small problem sizes.

We present elementary and efficient (mostly linear) algorithms for four fundamental problems: (1) finding the maximum reach value, (2) finding a maximum reach configuration (or enumerating all of them), (3) folding a given chain to a given maximum position, and (4) folding a chain in a way that changes the endpoint distance function monotonically. The algorithms rely on our recent theoretical results characterizing combinatorially the maximum of panel-and-hinge chains. They allow us to reduce the first problem to finding a shortest path between two vertices in an associated simple triangulated polygon, and the last problem to a simple version of the planar carpenter's rule problem.

1 Introduction

The *revolute-jointed robot arms* considered in this paper are spatial polygonal chains with fixed edge lengths and fixed angles between consecutive edges. The possible motions of the chain are rotations about the interior edges. These edges are called *revolute joints* or, when viewed as entire lines, *hinges*. As the robot arm moves between possible configurations, the distance between the two endpoints of the polygon (the *endpoint distance function*) takes on a continuum of values, of which the maximum one makes the focus of this paper. We remark that our chains are allowed to self-intersect during the motion. The following is a basic, long-standing open question in robotics, where it appears in connection with the much studied workspace computation problem [19, 3]:

The Maximum Reach Problem. *Given a 3D revolute-jointed robot arm, compute the maximum value of the endpoint distance function and a corresponding configuration.*

The main result of this paper is a *surprisingly simple, optimal, linear time algorithms for finding a maximum reach configuration for orthogonal chains,* and other classes (fully characterized by a technical condition). We show how to find the maximum value of the endpoint distance function, one of the (possibly exponentially many) maximum reach configurations, and how to fold to one of these configurations in a linear number of steps.

Although research on this problem spans over 40 years (see, e.g. [10, 8, 6, 1]), theoretical results contributed little to computational advances. The typical approach was based on formulating it as an optimization problem. In practice, for small-sized instances, it was solved with numerical approximation methods. Even very basic questions, such as whether a candidate solution can be *verified* in polynomial time, or whether the maximum is at all *computable* by a discrete algorithm, remained open. Indeed, in order to find the maximum, one has to look for it in a high dimensional space, described by the algebraic equations arising from the length and angle chain constraints. No *a priori* discrete underlying structure was known, to guide the search. For instance, if a gradient-based method landed in a potential well (local maximum), there was no theoretical criterion to distinguish a local maximum from the global one.

Papers studying the maximum reach of revolute jointed robotic manipulators have appeared in the robotics literature since at least 1969 [10], and gained momentum in the early 1980's, when a general, necessary condition satisfied by *all critical points* of the endpoint distance function was identified [8, 13, 19, 16]. An approximation method received in 1985 the ACM

[1] Department of Mathematics, Rider University, Lawrenceville, NJ 08648. *email:* borcea@rider.edu

[2] Department of Computer Science, Smith College, Northampton, MA 01063, USA. istreinu@smith.edu. streinu@cs.smith.edu,http://cs.smith.edu/~streinu.

[3] Research supported by a DARPA "23 Mathematical Challenges" grant, under "Algorithmic Origami and Biology".

Distinguished Dissertation Award [12]. Recent activity focuses on effectively finding or approximating the workspace boundary for *specific* mechanical manipulators with few joints [2, 1]. A strong impetus comes from the applications of robotics methods in Molecular Biology (see e.g. [5]).

Our Results. We present combinatorial algorithms for the following four fundamental problems on robot arm reachability, applied to orthogonal chains:

1. **Maximum Reach Value:** compute the maximum value of the endpoint distance function.
2. **Maximum Reach Configuration:** compute one (or all, when the number if finite) of the configurations that achieve the global maximum of the endpoint distance.
3. **Motion Planning:** given an arbitrary configuration of the chain, reconfigure it to a maximum reach position: i.e. compute a trajectory in configuration space ending at a specific maximum reach configuration.
4. **Optimized Motion Planning:** given a flat configuration, reconfigure it in such a way that the distance function increases towards the maximum throughout the motion.

The class of chains for which these algorithms work is actually larger, and fully characterized by a technical condition, related to the triangle inequality on the sphere. This will be described in Section 5. In particular, this holds for chains with all angles equal to α, for $\alpha \geq \frac{\pi}{3}$. However, in order to avoid cluttering the presentation with technicalities, we'll focus on the orthogonal case.

The main effort goes into solving problem (1). We do so with a linear time algorithm for computing not just the maximum reach value, but also the fold points and the fold pattern of the flat pieces of the corresponding configuration. After that, in linear time we compute the *angles* by which the panels will be rotated at the fold points. A maximum reach *configuration* is then computed in linear time by standard forward kinematics calculations. Similarly, problem (3) can be solved by designing a trajectory that sequentially rotates the panels by the appropriate angles. The solution to problem (4) relies on expansive motions, and will be briefly sketched at the very end. To stay within our goal of designing *combinatorial* algorithms whose complexity can be described in terms on n, we use the $O(n^3)$-events algorithm [17] for the planar Carpenter's Rule Problem.

Overview of the paper. We give the necessary definitions in Section 2, and state our previous theoretical results in Section 3. Along the way, we describe a structure theorem for maximum configurations, based on so-called rope segments and fold points, and present the equivalent shortest-path formulation which is more amenable to algorithmic treatment. The main algorithm appears in Section 4. It computes not just the length of the maximum reach, but also identifies, from a certain flat configuration, the structural elements of a maximal one. In Section 5, we describe the algorithm for computing a maximum reach configuration, which allows us to identify the technical condition which makes this process possible: the single-vertex origami folding. We now prove that the algorithm works correctly if and only if this condition is satisfied. In Section 7, we further refine the folding process to work in a manner that increases the endpoint distance monotonically. We conclude with some open problems.

2 Definitions

Revolute-jointed chains. A *robot arm* with n revolute joints (hinges) is given by a polygonal chain $p = \{p_0, p_1, \cdots, p_{n+2}\}$ in $3D$, with fixed edge lengths and fixed angles between consecutive edges. The hinges correspond to the internal edges $e_i = (i, i+1), i = 1, \cdots, n$. The two points $s = p_0$ and $t = p_{n+2}$ are referred to as the *endpoints* of the chain, with s being the *start* or *origin*, and t the *terminus* or *end point*. Another way to look at such a chain is as follows: the fixed angle constraint turns all triplets of vertices $p_i p_{i+1} p_{i+2}$ into rigid triangles, since the length of the edge $p_i p_{i+2}$ is implied by the other two and by the angle between them. The plane of the triangle is called a *panel*, and consecutive panels $p_i p_{i+1} p_{i+2}$ and $p_{i+1} p_{i+2} p_{i+3}$ are joined by the hinge e_{i+1} running through $p_{i+1} p_{i+2}$. *A reminder:* a hinge should be conceived as an entire line, not just a line segment.

Panel-and-hinge chains. More generally, a *panel-and-hinge chain* is a sequence of panels connected by hinges. A *panel* is a plane, and a *hinge* is a line, rigidly attached to it. In a chain, all panels have exactly two hinges, except for the two extreme ones which contain just one hinge each. Two consecutive panels are free to rotate, one relative to the other, around their common hinge. An *origin* or *start point* is fixed on the first panel, and an *end-point* or *terminus* is marked on the last.

Panel-and-hinge chains allow for the case of parallel consecutive hinges or several consecutive hinges incident in the same point, but a *generic* chain won't have such degeneracies. If we connect the start point to a point

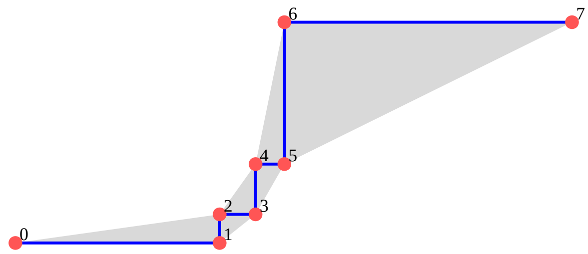

Figure 1: Rigid triangles in the panel-and-hinge chain associated to the revolute-jointed chain of Fig. 3(a).

on the first hinge by a line segment (an edge) and the terminus point to a point on the last hinge by another edge, we retrieve a revolute-jointed chain presentation with internal edges given by the segments on the hinges between two crossing points. The panels can be again conceived as triangles. See Fig. 1.

Endpoint axis and segment. The *line* (resp. line segment) joining the start and terminus is called the *endpoint axis* (resp. endpoint segment) of the chain.

Configuration space. The set of all possible spatial positions of the vertices which satisfy the edge length and angle constraints of a revolute-jointed chain (resp. panel-and-hinge), *up to rigid motions*, forms the *configuration space* of the chain. **We allow our chains to self-intersect**. The configuration space is naturally isomorphic to the n-dimensional torus $(S^1)^n$, for all the types of chains defined above. For panel-and-hinge chains, it can be parametrized by the dihedral angles between consecutive panels.

We emphasize that we address primarily the **generic** case in each class of chains. That means working on the complement of a proper algebraic subvariety of the parameter space of that class. Nevertheless, once a pattern is recognized, it is not difficult to see which aspects persist for the "non-generic" limit locus.

Flat configurations. When all the panels are coplanar, we say that the panel-and-hinge structure is in a *flat* configuration or simply *flat*. If the panels arise as triangles from a revolute-jointed polygonal chain, a special *standard* configuration is distinguished: when consecutive triangle do not overlap. Fig. 3 illustrates the standard *flat configuration* of an *orthogonal* chain (with equal right angles) having 5 hinges. Its panel-and-hinge representation from Fig. 1 illustrates the local non-overlapping property. More generally, it is easy to show that there is *no global overlap* for all chains with equal obtuse angles.

Endpoint (squared) distance. The *endpoint distance function* assigns a real non-negative value (the distance between the endpoints p_0 and p_{n+2}) to each spatial configuration of the chain. In fact, the squared distance function is more convenient for computations. The endpoint distance varies between two extreme values, the *global* minimum and maximum, with the possibility of various other local minima or maxima.

3 Theoretical background

The insufficient theoretical understanding of maximum configurations seems to be partially responsible for the lack of discrete (non-numerical) algorithms. A *necessary* condition for extremal non-zero [5] configurations was recognized and proven in several papers [8, 13, 19, 16]. In the words of [16], this necessary condition says: *"the line of sight from the base-point to the hand must intersect all turning axes"*[6], where the base-point may be chosen arbitrarily, the end-point is called "hand" and the "turning axes" are what we call hinges. However, all *critical points* with non-zero value for the squared distance function between the extreme points (not just the maxima) satisfy this condition.

Structure of critical configurations. As an immediate consequence of this condition, we obtain simple structural properties of panel-and-hinge chains in critical non-zero configurations. Two consecutive hinges may be met by the endpoint axis either in two distinct points (in which case, the axis lies in the plane, or panel, spanned by the two hinges), or in their intersection point; in this last case, the endpoint axis may not lie in the plane of the two hinges. If several consecutive hinges are met at distinct points, they (and consequently the panels they span) must be coplanar. Thus, the chain is subdivided into flat pieces (made by several consecutive coplanar panels cut by the endpoint axis), and connector panels. A connector panel is not coplanar with the endpoint axis. Instead, it meets the endpoint axis at the intersection of its two incident hinges. These special points, where the endpoint axis meets two (or more) concurrent hinges simultaneously, are called *fold points*.

In summary: the endpoint axis cuts across the hinges in the flat regions, and goes simultaneously through two consecutive hinges at fold points. See 8(b) for an example with two fold points; the endpoint axis meets three hinges in the middle region. *We will make*

[5] Configurations where the endpoint distance function is zero are also critical points, but they are not isolated for $n \geq 4$.

[6] This incidence of the origin-to-terminus line with the hinges is understood projectively, that is, it includes the possibility of parallelism.

substantial use of this property in the description of our algorithms.

Recently, in [4], we have extended this condition to a combinatorial, necessary and sufficient characterization of the Maximum Reach configurations. Because it helps to compare what is specific to the special case addressed in this paper, we state it in its full generality, for *body-and-hinge chains*. This is the most general class of serial robotic manipulators with revolute joints, defined as a collection of rigid *bodies* connected serially by hinges. The difference from panel-and-hinge chains is that the two hinges attached to each body (except the first and the last, which have only one hinge) need not be coplanar. As before, we mark two points, a *base* or *start point* on the first body, and an *end point*, or *terminus* on the last body, and ask for the maximum distance between them. The *natural order* of the hinges is $1, 2, 3, \cdots$ as they appear on the chain. See Fig. 2. We have the following *complete theoretical characterization* (valid in arbitrary dimension):

Theorem 3.1. *[4]* **(Global Maximum)** *A body-and-hinge chain is in a global maximum configuration if and only if the* oriented segment *from the origin s to the terminus t intersects all hinges* in their natural order.

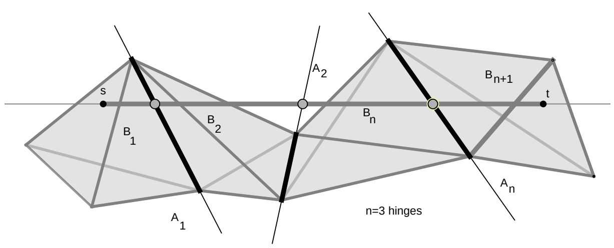

Figure 2: A body-and-hinge chain in R^3 with $n = 3$ hinges, 4 bodies (visualized as tetrahedra) and two marked points s and t on the end-bodies. In a maximum reach position, the axes meet the *oriented segment st* in the natural order.

Indeed, given a configuration satisfying this condition, we will mark in red the line segment from s to t, and think of its pieces, between the intersection points with the hinges, as being rigidly attached to the corresponding bodies. In any other configuration of the chain, the red path appears as a polygonal chain in 3D; hence the endpoint distance will be shorter than the length of the red path. The necessity of the condition is obtained from a characterization of the global maximum as a global minimum of another function:

Theorem 3.2. *[4]* **(Global Maximum as a Global Minimum)** *The global maximum of the endpoint distance function coincides with the length of the shortest path from s to t which meets all hinges in their natural order.*

See Fig. 3 for an example of a flat configuration which is, and one which is not a maximum, as witnessed by the pattern of intersection of the hinges with the endpoint axis. Notice that flat configurations are automatically critical points of the endpoint distance function, since the endpoint axis and all hinges are coplanar, and therefore projectively incident. Later on, Fig. 8 illustrates a flat, non-maximal configuration and a corresponding global maximum.

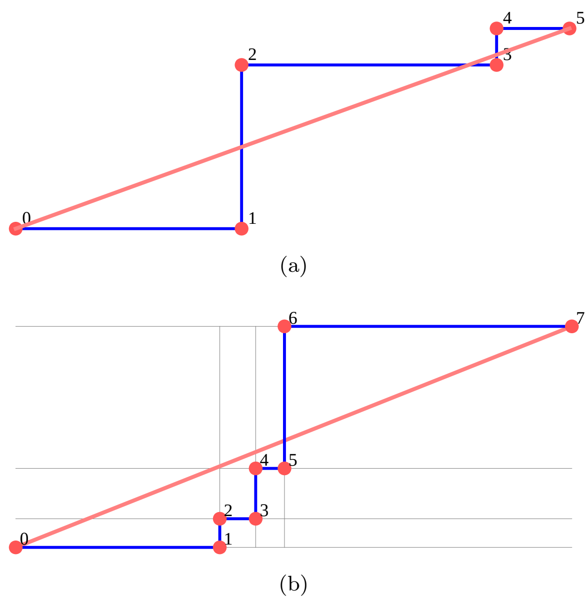

Figure 3: Illustration of Theorem 3.1. (a) This flat orthogonal chain is in its global maximum position, since the segment from the start to the terminus crosses the hinges in the natural order. (b) The hinges (in light gray) are crossed in a different order. The maximum reach requires a non-flat configuration in this case.

In this paper, we rely on these properties to devise the algorithms. The proofs of these Theorems have appeared in [4].

Notice that Theorem 3.1 immediately yields a simple linear time *verification algorithm* for the Maximum Reach. By contrast, the "classical" necessary condition of [8, 13, 19, 16] leads only to a verification procedure for being a *critical point*, not necessarily an maximum. The number of critical points of the endpoint distance function could be exponentially large, and - to the best of our knowledge - there is no known procedure that can isolate from them the maxima, based on this information alone. Theorem 3.2 is also an essential ingredient in our algorithm for Maximum Reach, since it allows us to reduce its calculation to a constrained shortest path problem.

As we said, critical configurations of panel-and-hinge chains are subdivided into flat pieces connected at *fold points*. When a panel-and-hinge chain is folded, the angles induced by the two incident hinges at a fold point and the constrained shortest path between the endpoints will satisfy a simple condition related to the triangle inequality on the sphere (this is a crucial condition; we'll say more about it later in the paper). At each fold point, the incident panels can be (generically) folded in two distinct ways (the applicable concept of genericity includes most of the polygonal chains). We obtain:

THEOREM 3.3. *[4]* **(Number of Extremal Configurations)** *Generically, the number of distinct configurations of panel-and-hinge chains attaining the maximum reach is 2^f, where f is the number of fold points. All maxima are global.*

By contrast, for body-and-hinge chains, the global maximum is generically achieved by a unique configuration, and there may be exponentially many local maxima.

This theorem clarifies our goals: we will aim at computing the maximum reach value (which is unique) but not *the* maximum reach configuration (which is not). We will settle to folding the chain to *one* of the maximum reach positions, characterized by a certain pattern of orientations at fold points. The theorem also explains the observed behavior of gradient-based numerical methods, since there are no local (non-global) maxima (this is valid for all polygonal chains with fixed edge lengths and angles, not just the orthogonal ones).

4 Finding the maximum reach

We are ready now to describe the main algorithm. It finds the *value* of the maximum reach and computes additional information which will be used, in the next section, to compute one of the (possibly exponentially many) configurations in which the maximum can be attained. The proof of correctness, for orthogonal chains, is also addressed in the next section.

Recall the structural decomposition of a chain in a critical, and in particular in a maximum reach position described in the beginning of Section 3: it consists in flat regions connected at *fold points* via connector panels. An example appears in Fig. 8(b).

Preview. To compute the maximum reach, our algorithm computes the fold points and flat pieces. *Folding* the chain to *one* of these maximum configurations can then be done by sequentially rotating along the two hinges of the connector panel at each fold point, for angles that can be computed in constant time using basic spherical geometry. We remark that the algorithms are valid for a larger class of chains, described in the next section by a quite technical condition related to the triangle inequality on the sphere; it is much easier to follow and illustrate them for orthogonal chains.

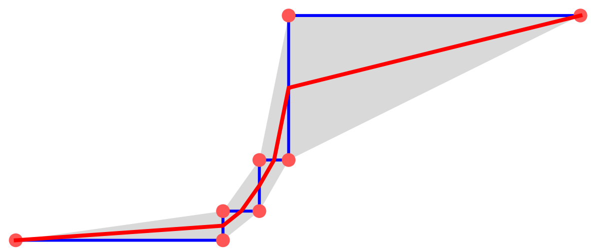

(a)

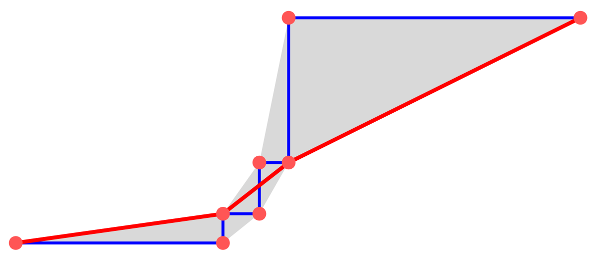

(b)

Figure 4: Finding the maximum reach for orthogonal chains. (a) The loose rope as a pseudoline inside the polygon. (b) The taut rope is the shortest path between the endpoints, and its length is the maximum reach.

Let us define the *polygon associated to a flat orthogonal chain in standard configuration* as the union of all triangles $p_ip_{i+1}p_{i+2}$, as in Fig. 1. Notice that the polygon interior, in gray in Fig. 1, is already triangulated by the chain *hinge segments* p_ip_{i+1}, $1 \leq i \leq n$.

Intuitively, imagine that we join the two endpoints by a loose rope and constrain it to meet all the hinge *segments* in *natural order*, as in Fig. 4(a), seeking to satisfy the condition of Theorem 3.1. In other words, we view the rope as a pseudo-line whose crossing pattern with the other lines is the natural order of the hinges. Then we pull the rope, while maintaining the chain flat and the rope confined inside the polygon. When the rope is taut, it becomes the *shortest (geodesic) path between the endpoints, inside the polygon*. If the path is a straight line, as in Fig. 3(a), it is the endpoint axis intersecting the hinges in natural order. If it is not straight, it bends at some chain vertices, as in Fig. 4(b). These are the *fold points*. Formally:

Algorithm 1. **Maximum reach and Fold Points**
Input: *A 3D orthogonal chain.*
Output: *The value of the maximum reach between the chain endpoints and the collection of* fold points.
Method:
[1]. In linear time, lay the chain flat in the standard configuration and compute the associated polygon.
[2]. Compute the shortest (geodesic) path between the chain endpoints lying inside the polygon.
[3]. Output the length of the shortest path: this is the maximum reach.
[4]. Output the sequence of vertices on the shortest path: these are the fold points.

To compute the geodesic path, we can use, for instance, the linear algorithms of [11] or [7]. This is convenient since the polygon comes with the triangulation given by the edges of the orthogonal chain.

If we can show that there is a 3D realization of the chain in which the shortest path computed by this algorithm, marked in *red* on the panel-and-hinge chain, aligns to a straight-line red segment, then the correctness of this algorithm follows from Theorem 3.1. Those cases in which this property (of having a 3D realization as described above) also illustrate a more restricted version of Theorem 3.2, one where the endpoint axis meets the *hinge segments* in the natural order. This is not true for more general chains, as illustrated in Fig. 5. Indeed, our algorithm, specialized to achieve this stronger condition, will *not* detect the maximum in *all* panel-and-hinge chains, e.g. for the example in Fig. 5. In the next section we characterize the class of chain for which this stronger property holds, and show that it includes the orthogonal chains.

5 Computing a maximum-reach configuration

We move now to the problem of computing a configuration attaining the maximum reach. Expanding upon the intuitive description given in the previous section, at the position where the rope is taut, we *freeze* the lengths of its segments. Each frozen rope segment may cross some chain edges, which will stay flat in any maximal configuration. We use this observation to construct an associated panel-and-hinge chain as follows: the hinges (of the original standard flat chain) crossed by each frozen rope segment are themselves frozen flat, and their plane becomes a single new panel. The hinges of the new chain are the hinges incident to the fold vertices (two at each vertex). Note that our new panel-and-hinge chain also

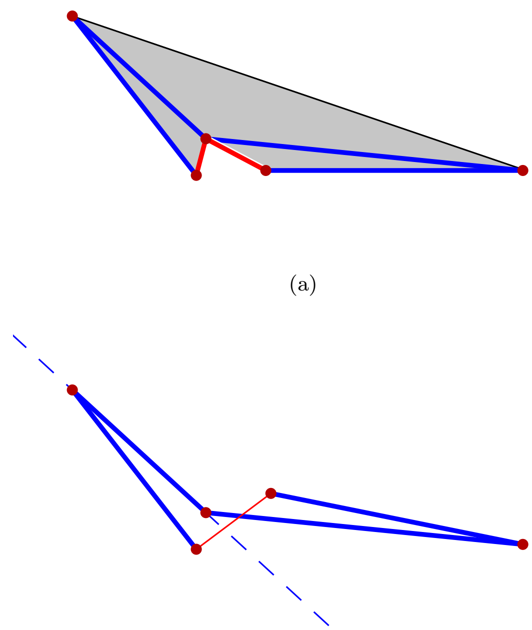

(a) (b)

Figure 5: A (non-orthogonal) chain on which Algorithm 1 does not apply. (a) The chain, in a standard flat position, with the shortest path computed by the algorithm; this is not, however, the global maximum reach. (b) The maximum reach is attained in a flat, non-standard (with locally overlapping panels) position, in which the endpoint segment (red) meets the hinges in natural order, but one of them is crossed *outside* the *hinge segment* region (dashed).

contains the (planes of the) triangles between the two hinges at a fold vertex. See Fig. 6(b).

We now seek to fold this new chain from its flat position to a spatial configuration where the frozen rope segments are aligned. This may not be always possible (for arbitrary chains). But we show that we can always decide easily *when* it is so, by verifying a simple technical property (defined below). Finally, we prove that orthogonal chains *always* satisfy this property.

The antipodal triangle inequality on the sphere. If we focus on one vertex of a panel-and-hinge chain, it has three panels and two hinges incident to it. This is visualized in Fig. 6(a). After the computation of the shortest path, a fold vertex is incident with two hinges and two segments of the frozen rope, as in Fig. 6(b).

At a fold vertex, the rope bends. This means that the three angles add up to more than π. The goal is to align the two rope segments by folding

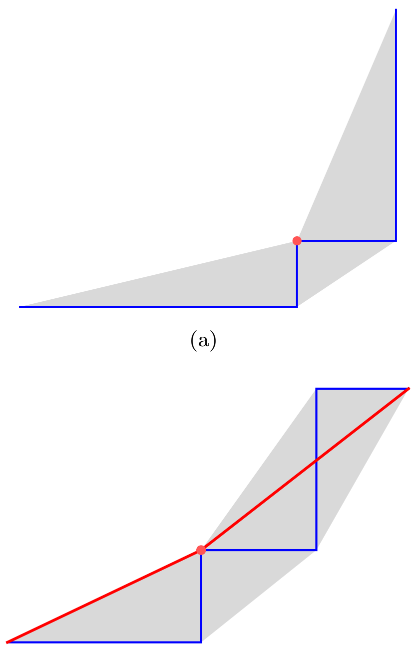

(a)

(b)

Figure 6: The three angles incident to a vertex, involved in the antipodal triangle inequality on the sphere, illustrated: (a) at a vertex of an orthogonal chain; (b) at a fold vertex, the three angles induced by the two red (frozen rope) and two blue (hinges) incident to the vertex. In this case, the two triangles crossed by the red line segment on the right become a new panel.

the simple three-edged *single vertex origami* of total spherical length between π and 2π (see [18, 14] for the relationship between spherical polygonal paths and single vertex origami). This cannot always be done, for instance when the three angles are $170, 30, 170$ degrees. A necessary and sufficient condition is given by the following Lemma.

Lemma 5.1. **(Antipodal Triangle Inequality)** *A spherical polygonal path of* 4 *vertices, made of three arcs of lengths* a, b, c *along the unit sphere, has a realization with antipodal endpoints iff the triplets of arc lengths* $a, b, \pi-c$ *and* $\pi-a, b, c$ *(and consequently also* $a, \pi-b, c$*) satisfy the triangle inequality.*

The spherical path with three arcs, in a position where its endpoints are antipodal, will be called an *antipodal spherical triangle.* See Fig. 7(b) for an example. The proof of the Lemma is elementary, since the triangle inequality must be satisfied for spherical triangles with edge lengths smaller than π, as well, and the antipodal triangle exists iff the complement $\pi - c$ of arc c (with respect to half of a great-circle)

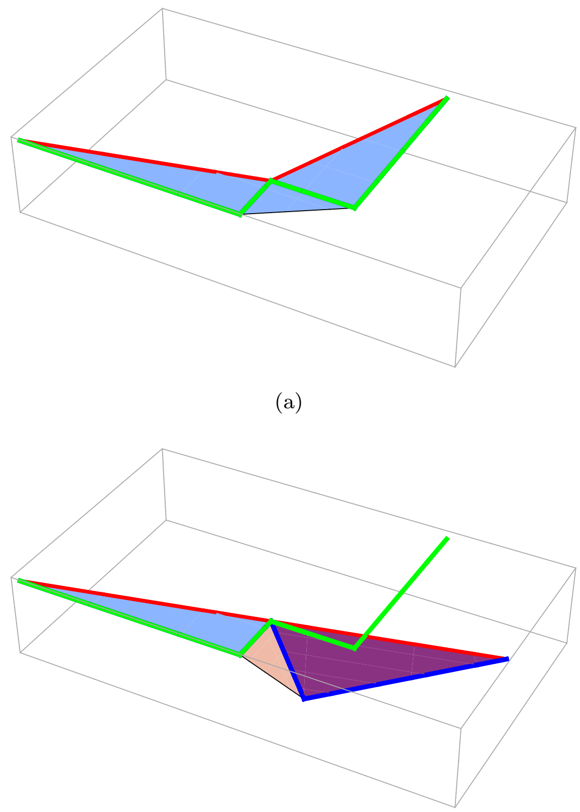

(a)

(b)

Figure 7: Folding three panels satisfying the Antipodal Triangle Inequality at a fold vertex. (a) The original flat configuration. (b) The final aligned fold. The taut rope in this position shows clearly that the maximum reach is obtained when its segments are aligned. The original flat chain contour is retained for visual reference.

forms a spherical triangle with the other two, iff the complement $\pi - a$ of arc a forms a spherical triangle with the other two. Elementary calculations show that the antipodal triangle inequality conditions lead to the following equivalent formulation:

Corollary 5.1. **Antipodal Triangle Criterion** *Three angles* a*,* b *and* c*, with* $0 < a, b, c < \pi$ *satisfy the antipodal triangle inequality iff they satisfy the following system of linear inequalities:*

$$a + b + c \geq \pi \tag{5.1}$$

$$a + b - c \leq \pi \tag{5.2}$$

$$a - b + c \leq \pi \tag{5.3}$$

$$-a + b + c \leq \pi \tag{5.4}$$

Using this criterion, we prove:

Corollary 5.2. *Chains with all equal angles α satisfy the* Antipodal Triangle Inequality *at every fold vertex iff $\alpha \geq \frac{\pi}{3}$. In particular, equal obtuse angles and orthogonal chains all fall into this category.*

Proof. We denote the three angles at a fold point as a, b and c, with b being the equal angle of the chain α, and use the criterion from Corollary 5.1. Notice first that $0 < a, c < \pi - b$: indeed, in the standard position of the chain, all sides follow just two directions (since the chain angles are equal), constraining the size of a and c to fall below $\pi - b$. The condition that the vertex is a fold point implies that the sum of the angles must exceed π, yielding condition (5.1). To verify (5.2) and (5.4), observe that $a+b-c < a+b < \pi-b+b = \pi$, and similarly for $-a+b+c$. Finally, $a-b+c < \pi-b-b+\pi-b = 2\pi-3b$, which is $\leq \pi$ exactly when $b \geq \frac{\pi}{3}$.

Theorem 5.1. **(Maximum reach via rope inside polygon)** *The maximum reach is the length of the end-to-end geodesic path inside the associated polygon iff each fold vertex satisfies the* antipodal triangle inequality on the sphere. *A maximum configuration is obtained by aligning the frozen rope segments at the fold points via folding the incident angle triplets to an antipodal spherical triangle.*

Proof. As we have observed in the Introduction, in any critical configuration the endpoint axis leads to the partitioning of the chain into flat pieces, connected at fold points (with a triangle in between). In a maximum reach configuration, the endpoint axis must meet the hinges in the natural order. At fold points, because of the alignment of the segments incident to the fold point, Lemma 5.1 applies. These statements hold in both directions for orthogonal chains.

Corollary 5.3. *The Maximum Reach of chains with all equal angles $\alpha > \frac{\pi}{3}$ is correctly computed by Algorithm 1.*

Finally, once we have computed the fold angles, we can fold the chain to a maximum configuration using a standard forward-kinematics robotics technique. For completeness, this is described in the next section.

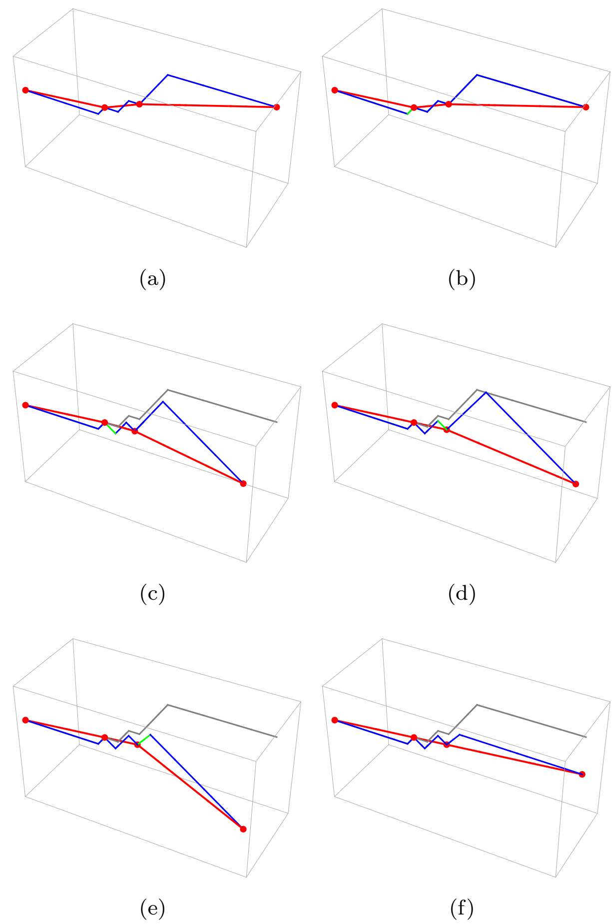

Figure 8: Folding a standard flat orthogonal polygon with two fold points to a maximum configuration. (a) The original flat configuration. (b)(c)(d)(e) With highlighted hinge, just before performing the corresponding rotation. (e) The final maximum fold. The original flat chain, in gray, is kept for visual reference. Notice the alignment of the rope segments in (d) and (f).

6 Motion Planning: folding to a maximum

The folding of the *single vertex origami* of three panels at each fold vertex into a position where the *frozen rope segments* become aligned is done sequentially via two rotations about the two hinges incident to the fold vertex. The alignment can be accomplished in one of two symmetric positions of the incident panels, which leads to an exponential number of possible configurations. Once we decide upon a desired fold pattern, then the entire folding process takes linearly many steps. Each folding step is a simple rotation of a part of the chain about one axis. The process of finding the final configuration becomes an instance of the classical forward kinematics problem for robotic manipulators.

ALGORITHM 2. **Folding to Maximum Reach**

Input: *A 3D orthogonal chain.*

Output: *A 3D configuration of the chain in maximum reach position.*

Method:

[1]. Using Algorithm 1, compute the fold points and the position of the frozen rope.

[2]. For each fold point, compute the two dihedral angles at the incident chain hinges, corresponding to the alignment of the incident frozen rope segments. Decide which of the two local folds is to be chosen, and encode them as signs for the dihedral angles.

[3]. For each hinge incident to a fold point, rotate the part of the chain containing the terminus by the angle computed at step [2].

A few steps in the folding algorithm are illustrated in Fig. 8.

Analysis. Step [1] takes linear time, and step [2] takes time linear in the number of fold points. Thus the complexity of the folding process, computed in terms of number of folding steps, is linear.

THEOREM 6.1. *A maximal configuration can be reached in a linear number of vertex folding steps.*

Continuous folding. Step [3] of the algorithm can be adapted in several ways to create a continuous motion. First, the folding can be simulated continuously one hinge rotation at a time. Second, *all* the hinge rotations can be distributed at each time step, and applied at the same speed to obtain a folding trajectory.

None of these two motions guarantees that the endpoint distance increases monotonically. We describe next a different motion planning strategy, which achieves this property.

7 Expanding the endpoint distance to maximum

In the motion planning algorithm described above, the distance between the endpoints may not vary monotonically towards the maximum value. This can be observed for instance in the motion from in Fig. 8. It is natural to ask whether one can design such a specialized motion not by pursuing a gradient-based numerical method, but based on a discrete algorithm.

We next show a modification of the continuous version of the Algorithm 2 discussed in the previous section, which accomplishes this via a reduction to the planar Carpenter's Rule problem.

THEOREM 7.1. *Starting from a planar standard configuration, a maximum-reach configuration can be attained in a manner that increases the endpoint distance throughout the motion.*

This is achieved by first applying the pseudo-triangulation roadmap algorithm of [17] to the *planar chain* determined by the frozen rope, in the plane of the first panel. The relative motion of two incident rope-segments is then used to determine the folding motion at each fold vertex.

ALGORITHM 3. **Monotone Folding to Max Reach**

Input: *A 3D orthogonal chain in a standard flat configuration, together with its fold points, frozen rope-segments and desired folding pattern at each fold vertex.*

Output: *A trajectory that folds the chain to a maximum configuration and expands the endpoint distance throughout the motion.*

Method:

[1]. In the plane of the initial flat configuration of the chain, compute an expansive motion of the polygonal chain given by the frozen rope using the second author's combinatorial algorithm [17] for the Carpenter's Rule Problem based on pseudo-triangulations. The trajectory consists in continuous motion intervals (called expansive intervals*) between two events which align two pseudo-triangulation edges.*

[2]. For each expansive interval, compute the single-vertex origami motion at all fold-vertices.

The algorithm has a subtlety in Step [2], since even with one endpoint fixed and another moving along a determined spherical trajectory, the single vertex origami has an additional degree of freedom. At the end of the folding, that degree of freedom disappears, potentially causing some numerical instability. The pseudo-triangulation algorithm of [17] achieves the straightening of the frozen rope (and thus a maximal-reach configuration) in at most $O(n^3)$ reconfiguration steps.

8 Concluding remarks

Our very simple and efficient algorithms are the first ones that have a chance to make some aspects of the computations involved in folding of *special families* of chains (not too dissimilar from the actual protein backbones) tractable. As such, we anticipate that our techniques may open a new direction in the study of robot arms and their biomechanical applications. Although, for keeping the presentation uncluttered, we have formulated our algorithms for *generic* chains, it is not hard to extend them for other situations, such as panel-and-hinge with more than four panels incident at one fold point; this extension is straightforward.

We conclude by formulating the following:

Conjecture: *There is a polynomial time, combinatorial algorithm for the Maximum Reach Problems, for general panel-and-hinge chains.*

We also conjecture that the problem is NP-hard for body-and-hinge chains, and emphasize that an NP-completeness would be an important theoretical advance for this case. So far no known methods, even approximate numerical ones, are guaranteed to compute the (generically unique) global maximum in this case: the gradient-based methods may get stuck in local maxima, and annealing methods may hop between local maxima with no criterion to guide them toward the global maximum. Note, however, that our natural-order criterion would allow these methods to decide, when in a local maximum, whether it is or not the global one.

Acknowledgment This research was sponsored by a DARPA "23 Mathematical Challenges" grant. All statements, findings or conclusions contained in this publication are those of the authors and do not necessarily reflect the position or policy of the Government. No official endorsement should be inferred.

References

[1] Karim Abdel-Malek, Jingzhou Yang, and Yunqing Zhang. On the workspace boundary determination of serial manipulators with non-unilateral constraints. *Robotics and Computer-Integrated Manufacturing*, 24:60–76, 2008.

[2] Karim Abdel-Malek, Harn-Jou Yeh, and Saib Othman. Interior and exterior boundaries to the workspace of mechanical manipulators. *Robotics and Computer Integrated Manufacturing*, 16:365–376, 2000.

[3] Jorge Angeles. *Fundamentals of Robotic Mechanical Systems: Theory, Methods and Algorithms*. Mechanical Engineering Series. Springer-Verlag New York, Inc., 2007.

[4] Ciprian S. Borcea and Ileana Streinu. Extremal configurations of manipulators with revolute joints. In *Reconfigurable Mechanisms and Robots, Proc. ASME/IFToMM International Conference (ReMAR'09), Jian S. Dai, Matteo Zoppi and Xianwen Kong (eds.), King's College, London, UK*, pages 279–284. KC Edizioni, June 2009. arXiv:0812.1375.

[5] John F. Canny and David Parsons. Geometric problems in molecular biology and robotics. In *Proceedings of the Second International Conference on Intelligent Systems for Molecular Biology, Stanford, CA*. August 1994.

[6] Marco Ceccarelli. A formulation for the workspace boundary of general n-revolute manipulators. *Mechanism and Machine Theory*, 31(5):637–646, 1996.

[7] Bernard Chazelle. A theorem on polygon cuttings with applications. In *Proc. 23rd Ann. Symp. on Foundations of Computer Science (FOCS)*, pages 339–349, 1982.

[8] Stephen Derby. The maximum reach of revolute jointed manipulators. *Mechanism and Machine Theory*, 16(3):255–261, 1981.

[9] Joseph Duffy. *Analysis of Mechanisms and Robot Manipulators*. Wiley, New York, 1980.

[10] Joseph Duffy and M. J. Gilmartin. Limit positions of four-link spatial mechanisms: mechanisms having revolute and cyllindric pairs. *Journal of Mechanisms*, 4:261, 1969.

[11] Leonidas J. Guibas, John Hershberger, Daniel Leven, Micha Sharir, and Robert Endre Tarjan. Linear-time algorithms for visibility and shortest path problems inside triangulated simple polygons. *Algorithmica*, 2(4):209–233, 1987.

[12] James Urey Korein. *A geometric investigation of reach*. MIT Press, Cambridge, MA, June 1985.

[13] A. Kumar and K. J. Waldron. The workspaces of a mechanical manipulator. *Journal of Mechanical Design*, 103(3):665–672, 1981.

[14] Gaiane Panina and Ileana Streinu. Flattening single-vertex origami: the non-expansive case. In *Proc. 25th Annual ACM Symposium on Computational Geometry*, pages 316–323, June 2009.

[15] Robert J. Schilling. *Fundamentals of Robotics*. Prentice Hall, 1990.

[16] R. G. Selfridge. The reachable workarea of a manipulator. *Mechanism and Machine Theory*, 18(2):131–137, 1983.

[17] Ileana Streinu. Pseudo-triangulations, rigidity and motion planning. *Discrete and Computational Geometry*, 34(4):587–635, November 2005.

[18] Ileana Streinu and Walter Whiteley. Single-vertex origami and spherical expansive motions. In Jin Akiyama and M. Kano, editors, *Proc. Japan Conf. Discrete and Computational Geometry (JCDCG 2004)*, volume 3742 of *Lecture Notes in Computer Science*, pages 161–173, Tokai University, Tokyo, 2005. Springer Verlag.

[19] K. Sugimoto and Joseph Duffy. Determination of extreme distances of a robot hand - Part 1 : A general theory. *Journal of Mechanical Design*, 103(3):631–636, 1981.